Journal of Pharmaceutical and Biomedical Analysis 145 (2017) 555–568

Contents lists available at ScienceDirect

Journal of Pharmaceutical and Biomedical Analysis

journal homepage: www.elsevier.com/locate/jpba

Characterization of the phase I and phase II metabolic profile of tolvaptan by *in vitro* studies and liquid chromatography–mass spectrometry profiling: Relevance to doping control analysis

Monica Mazzarino[a,*], Valeria Buccilli[a], Xavier de la Torre[a], Ilaria Fiacco[a], Amelia Palermo[a,b,1], Daniele Ughi[a], Francesco Botrè[a,c]

[a] *Laboratorio Antidoping, Federazione Medico Sportiva Italiana, Largo Giulio Onesti, 1, 00197 Rome, Italy*
[b] *Dipartimento di Chimica e Tecnologia del Farmaco, "Sapienza" Università di Roma, Piazzale Aldo Moro 5, 00185 Rome, Italy*
[c] *Dipartimento di Medicina Sperimentale, "Sapienza" Università di Roma, Viale Regina Elena 324, 00161 Rome, Italy*

ARTICLE INFO

Article history:
Received 1 April 2017
Received in revised form 19 June 2017
Accepted 23 June 2017
Available online 14 July 2017

Keywords:
Tolvaptan
In vitro metabolism
LC–MS/(MS)
Anti-Doping analysis
Drug-drug interactions
Azole antifungals

ABSTRACT

Phase I and phase II biochemical reactions involved in the biotransformation pathways of tolvaptan were characterized by LC–MS-based techniques and *in vitro* models to identify the most appropriate marker(s) of intake. The effects of physiological and non-physiological factors on the metabolic profile of tolvaptan were also evaluated. *In vitro* approaches were based on the use of pooled human liver microsomes and recombinant isoforms of cytochrome P450 and uridine diphospho glucuronosyl-transferase.

Sample preparation included liquid/liquid extraction at neutral pH with *tert*-butyl methyl-ether. In the case of the study of phase II metabolism an additional enzymatic hydrolysis step was performed. The chromatographic separation was carried out using reversed-phase chromatography, whereas detection was performed by either triple-quadrupole or time-of-flight analyzers in positive electrospray ionization and different acquisition modes.

Our data show that tolvaptan is metabolized to at least 20 phase I metabolites, the biotransformation reactions being catalyzed mainly by CYP3A4 and CYP3A5 isoforms. The phase-I reactions include hydroxylation (in different positions), carboxylation, oxidation, hydrogenation, dealkylation, isomerization and a combination of the above. Most of the phase I metabolites undergo glucuronidation, carried out mostly by UGT2B7 and UGT2B17 isoforms. Dealkylated, mono-hydroxylated and carboxylated metabolites both in the free and in the glucuronidated form appear to be the most suitable urinary diagnostic markers for the detection of tolvaptan intake in doping control. Concerning the effects of physiological and non-physiological factors on the metabolic profile of tolvaptan, our results show that (i) no significant gender differences were detected; (ii) significant differences were registered in the presence of different CYP3A5 allelic variants, and finally (iii) a marked reduction of the detected metabolites was registered in the presence of antifungals, and, to a lesser extent, of steroidal progestins.

1. Introduction

Vaptans are a relatively new class of pharmacologically active drugs designed and synthesized to overcome problems associated with the use of peptide arginine vasopressin antagonists. They selectively antagonize the action of vasopressin at its receptor subtypes V_1a, V_1b, and V_2 [1–3]. These receptors are distributed widely throughout the body and present a variety of functions, with the V2 receptors located in the distal collecting tubule of the kidney, and involved in the modulation of the antidiuretic action of arginine vasopressin [3–5].

The first orally active non-peptide selective vasopressin V2 receptor antagonist was OPC-31260 (mozavaptan) [6], followed by a more selective V2-receptor antagonist, OPC-41061 (tolvaptan, (N-{4-[(5RS)-7-chloro-5-hydroxy-2,3,4,5-tetrahydro-1H-benzo[b]azepin-1-carbonyl]-3-methylphenyl}2-methylbenzamide) [7]. Tolvaptan was developed by Otsuka Pharmaceutical Co., Ltd. (Tokyo, Japan), and approved by the U.S. Food and Drug Administration (FDA) in 2009 [8–11]. It acts to

* Corresponding author.
E-mail addresses: monica.mazzarino@fmsi.it, monica.mazzarino@gmail.com (M. Mazzarino).
[1] Present address: Institute of Molecular Systems Biology, ETH Zurich, Switzerland.

http://dx.doi.org/10.1016/j.jpba.2017.06.054
0731-7085/

increase the excretion of free water (aquaresis) without losses of electrolytes or worsening of the renal function [1,9–11]. Indeed, tolvaptan works by inhibiting the arginine vasopressin–induced water reabsorption in the kidney, competitively blocking the binding of arginine vasopressin to vasopressin V2 receptors [1,9–11]. For the above characteristics, tolvaptan is mainly used in therapy, when the treatment by classical diuretics is ineffective, for the treatment of euvolaemic and hypervolaemic hyponatraemia and for specific disorders such as cirrhosis and congestive heart failure [1,9–11].

In sport, athletes might, instead, choose to illicitly use tolvaptan and/or other selective vasopressin V2 receptor antagonists (e.g. lixivaptan, mozavaptan and satavaptan) for four main reasons: (i) to flush, by forced diuresis, other prohibited substances previously taken (ii) to increase the urinary flow, with the consequent dilution of the concentration of prohibited compounds in urine (iii) to relieve the water retention induced by long treatments with anabolic androgenic steroids, and finally (iv) to achieve acute weight loss, especially in those sports where athletes are competing in different weight categories [12,13]. For the above reasons, vaptans were included in 2014 in the section S5 "Diuretics and masking agents" of the list of substances and methods that are prohibited in sport by the World Anti-Doping Agency (WADA) [14]. It has to be highlighted that whenever a new class of substances is included in the aforementioned list, the primary activity of the WADA-accredited anti-doping laboratories is to develop and to validate effective analytical strategies for the detection of the newly prohibited drug(s). Each analytical method has to be applied worldwide, under ISO 17025 accreditation, by all WADA-accredited laboratories. Clearly, apart from the analytical aspects, the knowledge of the metabolism/degradation and of the rate and route of elimination of any new doping drug is necessary to select the most appropriate biological fluid, timing of sample collection, and diagnostic marker(s) to identify the illicit use of the prohibited drug. The analytical target, provided it is excreted as such in detectable amounts and for a sufficiently long period, can be the parent drug itself, one (or more) of its metabolites, in the case the drug undergoes an extensive metabolic biotransformation before being excreted; or finally, the drug itself and one (or more) of its metabolites, if the drug undergoes a moderate biotransformation before being excreted.

Based on the above, a preliminary literature search revealed that tolvaptan is rapidly absorbed after oral intake. After administration of therapeutic doses (usually in the range 15–30 mg a day), its plasma concentration reaches the maximal values after 2–3 h and then decreases in an exponential way, being completely cleared from the body within the first 24 h [15–18]. In addition to this, tolvaptan is also highly bound to plasma proteins (80–99%) and the elimination occurs mainly in the faeces, with 10–40% of the administered dose excreted in the urine (1% as parent compound, the rest as metabolites) [15–18]. Literature data indeed report that tolvaptan is extensively biotransformed in the liver via CYP3A4 isoenzyme to form oxidized, carboxylated and hydroxylated metabolites. Furukawa et al. [19] described nine phase I metabolites of tolvaptan (an oxidized metabolite, three hydroxylated metabolites on the benzazepine ring, a hydroxylated oxidized metabolite, a hydroxylated metabolite with a cleaved benzazepine ring, a hydroxylated oxidized metabolite with a cleaved benzazepine ring and two carboxylated metabolites) in rat serum. Rzeppa et al., focusing on the same nine metabolites, reported that after the intake of a single dose of tolvaptan (15 mg, Samsca™) by one male subject, the most abundant compounds found in urine were the hydroxylated and the carboxylated metabolites [20]. To the best of our knowledge, no similar data are yet available on phase II metabolism.

Gender depending differences were also reported in the serum concentration–time profiles for tolvaptan and its metabolites in rats: the carboxylated oxidized metabolite was found in higher levels than tolvaptan in male rats, whereas this evidence was reversed in female rats, where the serum concentration of tolvaptan was found to be higher than that of its main metabolites [19]. To the best of our knowledge, no similar data are yet available in humans.

Due to the scarce information regarding the metabolism of vaptans, we aimed to extend data on the phase I metabolic profile of tolvaptan and to investigate phase II metabolism with the aim to identify class-specific metabolic pathways and design a methodological approach to apply also to the study of the metabolism of other vaptans and consequently to develop appropriate analytical procedures to detect them in human urine. Alterations in the activity of the enzymatic systems involved in the metabolic reactions of tolvaptan as a consequence of physiological (gender and genetic polymorphism) or non-physiological (metabolic drug-drug interactions) factors were also considered, to assess the potential changes of the metabolic profile both from a qualitative point of view (i.e. formation of different metabolites) and from a quantitative one (amount/time of production of the different metabolites) [21–23,29–32]. This information will be useful to further refine the selection of the most appropriate marker(s) of administration also in the presence of potential confounding factors (e.g., antifungals) [21–23].

Given the difficulty in obtaining permission to perform excretion studies on humans (and especially those involving the co-administration of two or more active principles), our experiments were based on *in vitro* approaches, using human liver microsomes (HLM) and/or isolated cytochrome P450s (CYP) and uridine diphospho glucuronosyl transferase (UGT) recombinant isoforms. The metabolic profile of tolvaptan, either in the absence or in the presence of other pharmacologically active compounds, was finally characterized by LC–MS/MS, using triple quadrupole and/or time of flight mass analyzers in different acquisition modes.

2. Experimental

2.1. Chemicals and reagents

The pharmacologically active compounds tested in this study (i.e. tolvaptan, ketoconazole, econazole, miconazole, tioconazole, gestodene, levonorgestrel, and relcovaptan, used as internal standard) were all supplied by Sigma-Aldrich (Milano, Italy).

The reagents (formic acid, acetic acid, ammonium formate, ammonium acetate, sodium phosphate, sodium hydrogen phosphate, acetonitrile, methanol, dimethylsulfoxide (DMSO) and *tert*-butyl methyl-ether) were all of analytical grade and provided by Sigma-Aldrich (Milano, Italy). The ultrapurified water used was of Milli-Q-grade (Millipore Italia, Vimodrone, Milano, Italy).

The enzyme β-glucuronidase (from *E. coli*) used for the enzymatic hydrolysis of glucurono-conjugates, was purchased from Roche (Monza, Italy).

The enzymatic proteins (all UGT and CYP recombinant isoforms, as well as all HLM, these being those pooled from 20 Caucasian mixed male and female donors of different ages, those from female donors only and those from male donors only), as well as all the reagents (sodium phosphate and tris-HCl buffers, magnesium chloride hexahydrate, uridine 5′-di-phospho-α-D-glucuronic acid, alamethicin, glucose-6-phosphate, glucose-6-phosphate dehydrogenase, nicotinamide adenine dinucleotide phosphate and CYP450 oxidoreductase) used for the *in vitro* metabolism experiments were purchased from BD Biosciences (Milano, Italy). HLM containing the different CYP3A5 allelic variants (without activity CYP3A5 *3*3,

moderate activity CYP3A5 *1*3 and high activity CYP3A5 *1*1) were purchased from XenoTech (Kansas City, USA).

The single recombinant enzymatic isoforms considered in this study were the following: for the phase I (CYP-catalzyed) metabolism CYP1A2, CYP3A4, CYP3A5, CYP2B6, CYP2C8, CYP2C9, CYP2C19 and CYP2D6; and for the phase II (UGT-catalyzed) metabolism UGT1A1, UGT1A3, UGT1A4, UGT1A6, UGT1A7, UGT1A8, UGT1A10, UGT2B4, UGT2B7, UGT2B10, UGT2B15 and UGT2B17.

2.2. Protocols for the in vitro studies

2.2.1. Phase I metabolism

All incubation conditions were preliminarily optimized (proteins and substrate concentrations, buffer and solvent types, incubation times). Different solvents (methanol, DMSO and acetonitrile), buffers (phosphate and tris-HCl), pH values (5.0, 7.4, 8.0), concentrations of tolvaptan (1, 5, 10, 20, 30 40, 60, 80, 100, 150 and 200 μM) and of the enzymatic proteins (0.1, 0.2, 0.5 and 1.0 mg/mL), and different incubation times (30, 60, 120, 240, 480 and 720 min) were evaluated. The final incubation medium also contained 3.3 mM magnesium chloride, 1.3 mM $NADP^+$, 3.3 mM glucose-6-phosphate and 0.4 U/mL glucose-6-phosphate dehydrogenase in a total volume of 250 μL. Samples were pre-warmed at 37 °C for 5 min and the phase I reactions were started with the addition of the appropriate enzymatic proteins (either HLM or CYP recombinant isoforms). After incubation at 37 °C, 250 μL of ice-cold acetonitrile were added to stop the phase I reactions. The samples were then transferred into an ice bath for further precipitation of the proteins in the assay medium. The precipitate was subsequently separated from the supernatant by centrifugation at 21,000*g* (15,000 rpm) at room temperature for 10 min. Each set of assays also included a negative control sample, containing all reaction mixture components except the enzymatic proteins, to monitor the potential non-enzymatic reactions within the incubation period. Each incubation was processed in triplicate.

2.2.2. Phase II metabolism

To study glucuronidation reactions, 8 mM magnesium chloride and 25 μg/mL of alamethicin were added to the phase I reaction mixture described above. The phase I reactions were then initiated by adding HLM. After 10 min at 37 °C, 2 mmol of the cofactor uridine 5′-di-phospho-α-D-glucuronic acid were added and the phase II metabolism was run at 37 °C. The overall reaction was terminated by the addition of 250 μL of ice-cold acetonitrile. The samples were then transferred into an ice bath for further precipitation of the proteins in the assay medium. The precipitate was subsequently separated from the supernatant by centrifugation at 21,000*g* (15.000 rpm) at room temperature for 10 min. Each incubation was processed in triplicate.

To characterize the UGT isoenzymes involved in the phase II metabolism of tolvaptan, the metabolites formed using the phase I protocol reported above were extracted and incubated in 250 μL of 100 mM phosphate buffer (pH 7.4) containing 8 mM of magnesium chloride, 25 μg/mL of alamethicin and 2 mM of the cofactor uridine 5′-di-phospho-α-D-glucuronic acid. The reactions were initiated by adding the UGT recombinant isoforms considered in this study separately. The reaction medium was then incubated at 37 °C. The overall reaction was terminated by the addition of 250 μL of ice-cold acetonitrile. The samples were then transferred into an ice bath for further precipitation of the proteins in the assay medium. The precipitate was subsequently separated from the supernatant by centrifugation at 21,000*g* (15,000 rpm) at room temperature for 10 min. All incubations were performed in triplicate.

2.3. Sample preparation for the instrumental analysis

Sample pre-treatment was based on protocols already used in our laboratory to perform routine analyses [24]. Briefly, to the samples obtained by the *in vitro* experiments, 1.5 mL of phosphate buffer (1 M, pH 7.4), 50 μL of the internal standard (ISTD: solution of relcovaptan 10 μg/mL) were added and the liquid/liquid extraction was carried out with 7 mL *tert*-butylmethyl ether for 6 min on a mechanical shaker. After centrifugation the organic layer was transferred to a 10 mL tube and evaporated to dryness under nitrogen stream at 25 °C. The residue was reconstituted in 50 μL of mobile phase and an aliquot of 10 μL was injected on the liquid chromatography-mass spectrometry systems (for the detection of phase I metabolites).

In the case of phase II metabolism studies, samples were also subject to an enzymatic hydrolysis step: to the aqueous layer 50 μL of β-glucuronidase from *E. coli* and 50 μL of the internal standard (ISTD: solution of relcovaptan10 μg/mL) were added and the sample was incubated for 1 h at 55 °C. After hydrolysis, 7 mL of *tert*-butylmethyl ether were added and the liquid/liquid extraction was carried out for 6 min on a mechanical shaker. After centrifugation, the organic layer was transferred to a 10 mL tube and evaporated to dryness under nitrogen stream at 25 °C. The residue was reconstituted in 50 μL of mobile phase and an aliquot of 10 μL was injected on the liquid chromatography-mass spectrometry system.

2.4. Instrumental analysis

2.4.1. Liquid chromatography conditions

All LC experiments were performed using an Agilent 1200 Rapid Resolution Series HPLC pump with binary gradient system and automatic injector (Agilent Technologies S.p.A, Cernusco sul Naviglio, Milano, Italy). Reversed-phase liquid chromatography was performed evaluating different mobile phases compositions (methanol/water or acetonitrile/water) and modifiers (formic or acetic acid and ammonium formate or acetate), column temperatures (20, 30, 40 and 60 °C), lengths (5, 10 and 15 cm) and particle characteristics and sizes (5, 3.5 and 2.7 μm).

2.4.2. Triple quadrupole conditions

Experiments were performed using a triple quadrupole instrument (API4000 ABSciex, Monza, Italy) with positive and negative electrospray ionization (ESI). The experiments were performed using multiple reaction monitoring (MRM) as acquisition mode, employing collision-induced dissociation (CID) using nitrogen as collision gas at 5.8 mPa, obtained from a dedicated nitrogen generator system (Parker-Balston model 75-A74, CPS Analitica Milano, Italy) ensuring gas purity at 99.5% or higher. The mass spectrometric parameters (declustering and needle voltages, gases pressure, source temperature, collision cell exit potential and collision energy) were optimized by infusion of the standard solution of tolvaptan at a concentration of 10 μg/mL. To this purpose, a 1 mL syringe operated by a syringe pump at a flow-rate of 10 μL/min was utilized. All aspects of instrument control, method setup parameters, sample injection and sequence operation were controlled by the Analyst software version 1.6.1.

2.4.3. Time-of-flight (TOF) conditions

High-resolution/high-accuracy measurements were performed on an Agilent Technologies 6520 orthogonal acceleration time-of-flight mass spectrometer (Agilent Technologies S.p.A, Cernusco sul Naviglio, Milano, Italy), equipped with an electrospray ionization (ESI) source operating in positive and negative ion mode. Nitrogen was used as the drying and nebulising gas. The drying gas flow rate and temperature were 10 L/min and 350 °C, respectively. The nebulizer gas pressure was 45 psi. The applied capillary and the

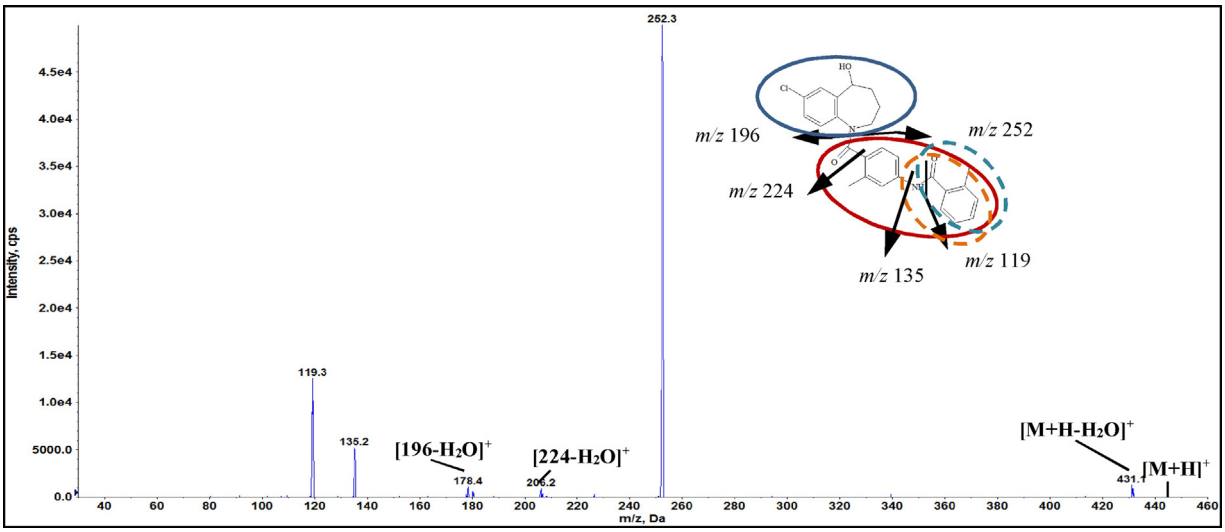

Fig. 1. Product ion spectrum, molecular structure, fragmentation pathways and structural markers of tolvaptan at a collision energy of 35 eV.

fragmentor voltages were optimized by infusion of the standard solution of tolvaptan at a concentration of 10 μg/mL. For this purpose, a 1 mL syringe operated by a syringe pump at a flow-rate of 10 μL/min was utilized. Mass spectral data were collected from *m/z* 100 to 1100 at 9300 transients per second. All other MS parameters (transfer optic voltage, voltage of the ion focus and octapole lens, TOF voltages, and detector voltage) were automatically optimized by the daily-performed instrument autotuning procedure. The mass calibration was also performed daily before starting the analysis using a calibration solution provided by the manufacturer.

Purine with an $[M+H]^+$ ion at *m/z* 121.0509 and an Agilent proprietary compound (HP0921) yielding an ion at *m/z* 922.0098 were simultaneously introduced via a second orthogonal sprayer, and these ions were used as internal calibrants along all the analysis. All aspects of instrument control, tuning, method setup and parameters, sample injection and sequence operation were controlled by the Agilent Technologies Mass Hunter software version B.02.01.

3. Results and discussion

3.1. LC–MS(/MS)

3.1.1. Mass spectrometric conditions

Instrumental parameters in MS and MS/MS were optimized by infusing the standard of tolvaptan dissolved in the mobile phase at a concentration of 10 μg/mL.

The full-scan MS analysis was first performed, both in positive and negative ionization modes, to identify and to optimize the conditions for the acquisition of the molecular ion. While no signals were obtained in full scan spectrum acquired in negative mode, abundant signal was recorded in positive mode for the protonated molecular ion $[M+H]^+$ at *m/z* 449. The signal of the protonated molecular ion was then optimized evaluating different mass spectrometric parameters. For the time-of flight system the best conditions were obtained using a fragmentor voltage of 175 V, an ion source temperature of 350 °C, a capillary voltage of 4000 V, a nebulizer gas pressure of 45 psi and a flow of the drying gas of 10 L/min. For the triple quadrupole, optimal results were obtained using a curtain gas pressure of 25 psi, a source temperature of 500 °C, an ion source gas 1 (auxiliary gas) pressure of 35 psi, an ion source gas 2 (nebulizer gas) pressure of 40 psi, a declustering voltage of 60 V, and a needle voltage of 5500 V.

Subsequently, MS/MS experiments were carried out at different collision energies (25, 30, 35, 40, 45, 50 and 60 eV) to obtain information about the fragmentation patterns of tolvaptan and to select representative structural markers. The protonated molecular ion $[M+H]^+$ undergoes extensive fragmentation also at the lowest collision energy tested, as result of the amide bridge cleavage between the benzazepine core and the rest of the molecule, leading to the formation of an abundant fragment ion at *m/z* 252 and of a minor fragment ion at *m/z* 178 (see Fig. 1). At higher collision energy, fragment ions corresponding to the cleavage at level of the methyl-benzamide portion were also detected at *m/z* 119 and 135 (see again Fig. 1).

3.1.2. Chromatographic conditions

In parallel to the development of the mass spectrometric acquisition methods, the chromatographic separation was optimized to ensure proper discrimination of the unknown compounds and other peaks from the background, and to obtain a good resolution between compounds that show the same precursor ion and fragmentation pattern, such as for example the mono-hydroxylated metabolites of tolvaptan. Different mobile phases composition (methanol/water or acetonitrile/water), mobile phase modifiers (formic or acetic acid and ammonium formate or acetate), column temperatures (20, 30, 40 and 60 °C) and column length (5, 10 and 15 cm) and particle characteristics and sizes (5, 3.5 and 2.7 μm) were evaluated. The best selectivity, sensitivity and peak shape were obtained using a column length of 10 cm with internal diameter of 2.1 mm and particle size of 2.7 μm, a column temperature of 40 °C, acetonitrile and water as mobile phase solvents and 0.1% of formic acid as mobile phase modifier. The selected gradient program started at 10% B and increased to 30% B in 10 min, after 4 min, to 40% B, after 3 min, to 60% B in 5 min, and then after 4 min to 100% B. The flow rate was set at 0.25 mL/min and the column temperature at 40 °C.

Fig. 2B shows the extract chromatogram obtained analyzing the sample obtained incubating tolvaptan in the presence of HLM, under the optimized chromatographic conditions. As it can be seen, a satisfactory separation between compounds with the same precursor ion and fragmentation pattern was obtained (see Table 1 for the selected precursor ions).

3.2. Development of the in vitro protocols

The *in vitro* phase I metabolism protocol was optimized considering the data already reported in literature [25–27] and the protocols already utilized in our laboratory to study drug

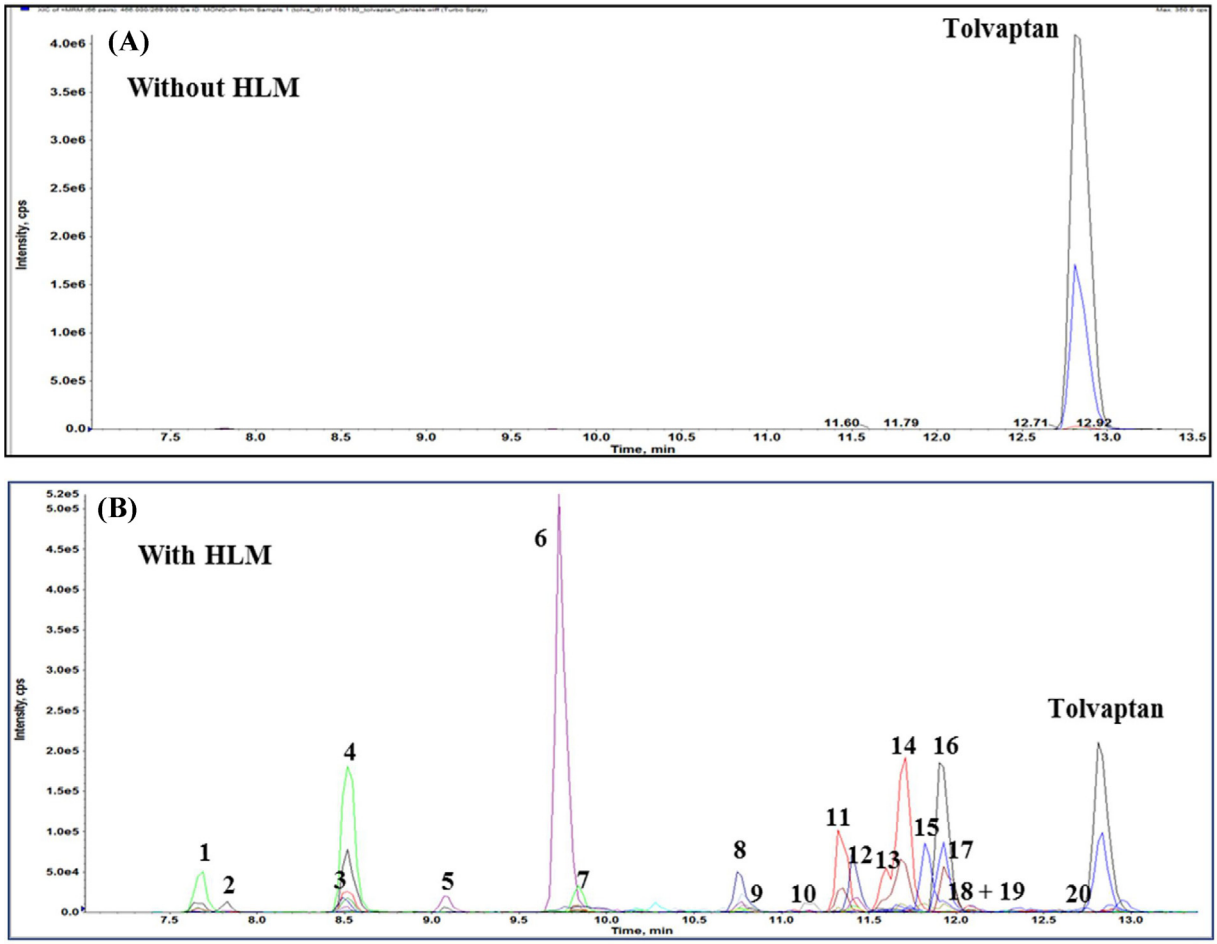

Fig. 2. Extracted chromatograms obtained analyzing *in vitro* samples after incubation of tolvaptan in the absence (A) and in the presence (B) of human liver microsomes. Detection was performed using the SRM method set up in this study. Peak identification: 1. *N-dealkylated mono-hydroxylated metabolite, 2. N-dealkylated mono-hydroxylated (cleaved benzazepine ring) metabolite, 3. N-dealkylated metabolite, 4. N-dealkylatedmono-hydroxylated metabolite, 5. N-dealkylatedmono-hydroxylated (cleaved benzazepine ring) metabolite, 6. N-dealkylated metabolite, 7. N-dealkylated mono-hydroxylated metabolite, 8. N-dealkylated carboxylated (cleaved benzazepine ring) metabolite, 9. N-dealkylated carboxylated (cleaved benzazepine ring) oxidized metbolite, 10. N-dealkylatedoxidized metabolite, 11. mono-hydroxylated metabolite, 12. carboxylated(cleaved benzazepine ring) metabolite, 13. mono-hydroxylated metabolite, 14. mono-hydroxylated metabolite, 15. mono-hydroxylated dehydrogenated (cleaved benzazepine ring) metabolite, 16. isomerization, 17. mono-hydroxylated (cleaved benzazepine ring) metabolite, 18. mono-hydroxylated (cleaved benzazepine ring) metabolite, 19. carboxylated (cleaved benzazepine ring) oxidized metabolite, 20. Oxidized metabolite*.

metabolism [28–30]. In details, to obtain a good correlation with the *in vivo* metabolism data available in the literature [19,20], we comparatively evaluated different experimental conditions, using different solvents (methanol, DMSO and acetonitrile), buffers (phosphate and tris-HCl) and pH values (5.0, 7.4, 8.0), as well as varying the concentration of substrate (1, 5, 10, 20, 30, 40, 60, 80, 100, 150 and 200 μM) and of the enzymatic proteins (0.1, 0.2, 0.5 and 1.0 mg/mL), and finally varying also the incubation time (30, 60, 120, 240, 480 and 720 min). In addition, to minimize the effect of intra-individual variation and to present an "average enzyme activity", the microsomal preparations selected in this study were obtained from a pool of 20 Caucasian mixed male and female donors of different ages.

The best results were obtained using as substrate solvent DMSO (the total amount of DMSO in the final assay was 1%), a substrate concentration of 20 μM, a proteins concentration of 0.5 mg/mL, phosphate buffer 0.1 M at pH 7.4, and an incubation time of 2 h.

Fig. 2A–B report the extracted chromatograms of samples obtained after the incubation of tolvaptan in the absence (Fig. 2A) and in the presence (Fig. 2B) of HLM. Twenty compounds not detected in the sample incubated in the absence of HLM were identified, including those (hydroxylated and carboxylated) described by Rzeppa et al. [20], thus confirming that the *in vitro* protocol and the analytical procedures set up in this study can be used to reliably reproduce the metabolic profile of tolvaptan in human.

3.3. Characterization of the phase I and II biotransformation pathways of tolvaptan

The samples from the *in vitro* assays were first analyzed by the time-of flight system in full scan acquisition mode to obtain information about the elemental composition of the compounds formed after the incubation of tolvaptan with HLM. Samples were then analyzed by the triple quadrupole system in MRM acquisition mode to detect the metabolites produced in low concentration and not detectable using the time-of flight system, as well as to obtain additional structural information. Being the metabolites of tolvaptan not available in our laboratory, the ion transitions utilized to develop the MRM method (see Table 1 for the ion transitions selected for tolvaptan and its metabolites) were obtained by calculating the protonated molecular ion $[M+H]^+$ of the potential tolvaptan metabolite (postulated after *in silico* investigation) and by selecting the characteristic fragmentation routes found in the product ion spectrum of tolvaptan (see Fig. 1), assuming a similar fragmentation behavior also for the phase I metabolites.

Table 1
Elemental composition, molecular weight, retention times (Rts), precursor ions and characteristic ion fragments.

ID	Compound	Elemental composition	MW (Da) (calc)	MW (Da) (exp)	Error (Δppm)	Rt (min)	Precursor ion (*m*/*z*)	Ion fragments (*m*/*z*)
M1	*N-dealkylation mono-hydroxylation*	$C_{18}H_{19}ClN_2O_3$	346.1084	346.1086	0.5	7.6	347	134; 194
M2	*N-dealkylation mono-hydroxylation (cleaved benzazepine ring)*	$C_{18}H_{21}ClN_2O_3$	348.1241	348.1227	1.7	7.7	349	134; 196
M3	*N-dealkylation*	$C_{18}H_{19}ClN_2O_2$	330.1135	330.1128	2.1	8.5	331	134; 178
M4	*N-dealkylation mono-hydroxylation*	$C_{18}H_{19}ClN_2O_3$	346.1084	346.1080	1.2	8.6	347	134; 194
M5	*N-dealkylation mono-hydroxylation(cleaved benzazepine ring)*	$C_{18}H_{21}ClN_2O_3$	348.1241	348.1248	2.0	9.1	349	134; 196
M6	*N-dealkylation*	$C_{18}H_{19}ClN_2O_2$	330.1135	330.1130	1.5	9.7	331	134; 178
M7	*N-dealkylation mono-hydroxylation*	$C_{18}H_{19}ClN_2O_3$	346.1084	346.1086	0.5	9.8	347	134; 194
M8	*N-dealkylation carboxylation (cleaved benzazepine ring)*	N.D.	N.D.	N.D.	N.D.	10.7	363	134
M9	*N-dealkylation carboxylation oxidation (cleaved benzazepine ring)*	N.D.	N.D.	N.D.	N.D.	10.8	361	134
M10	*N-dealkylation oxidation*	N.D.	N.D.	N.D.	N.D.	11.2	329	134
M11	*Mono-hydroxylation*	$C_{26}H_{25}ClN_2O_4$	464.1503	464.1500	0.9	11.3	465	194; 252
M12	*Carboxylation (cleaved benzazepine ring)*	$C_{26}H_{25}ClN_2O_5$	480.1452	480.1459	1.5	11.4	481	252
M13	*Mono-hydroxylation*	$C_{26}H_{25}ClN_2O_4$	464.1503	464.1508	1.1	11.6	465	194; 252
M14	*Mono-hydroxylation*	$C_{26}H_{25}ClN_2O_4$	464.1503	464.1508	1.1	11.7	465	194; 252
M15	*Mono-hydroxylation oxidation (cleaved benzazepine ring)*	$C_{26}H_{25}ClN_2O_4$	464.1503	464.1495	1.7	11.8	465	252
M16	*Isomerization*	$C_{26}H_{25}ClN_2O_3$	448.1554	448.1548	1.3	11.9	449	119; 135; 178; 252
M17	*Mono-hydroxylation (cleaved benzazepine ring)*	$C_{26}H_{27}ClN_2O_4$	466.1659	466.1650	1.9	12.0	467	252
M18	*Mono-hydroxylation (cleaved benzazepine ring)*	$C_{26}H_{27}ClN_2O_4$	466.1659	466.1662	0.6	12.1	467	252
M19	*Carboxylation oxidation (cleaved benzazepine ring)*	N.D.	N.D.	N.D.	N.D.	12.1	479	252
M20	*Oxidation*	$C_{26}H_{23}ClN_2O_3$	446.1397	446.1392	1.1	12.7	447	119; 135; 178; 252
P	*Tolvaptan*	$C_{26}H_{25}ClN_2O_3$	448.1554	448.1559	1.1	12.8	449	119; 135; 178; 252

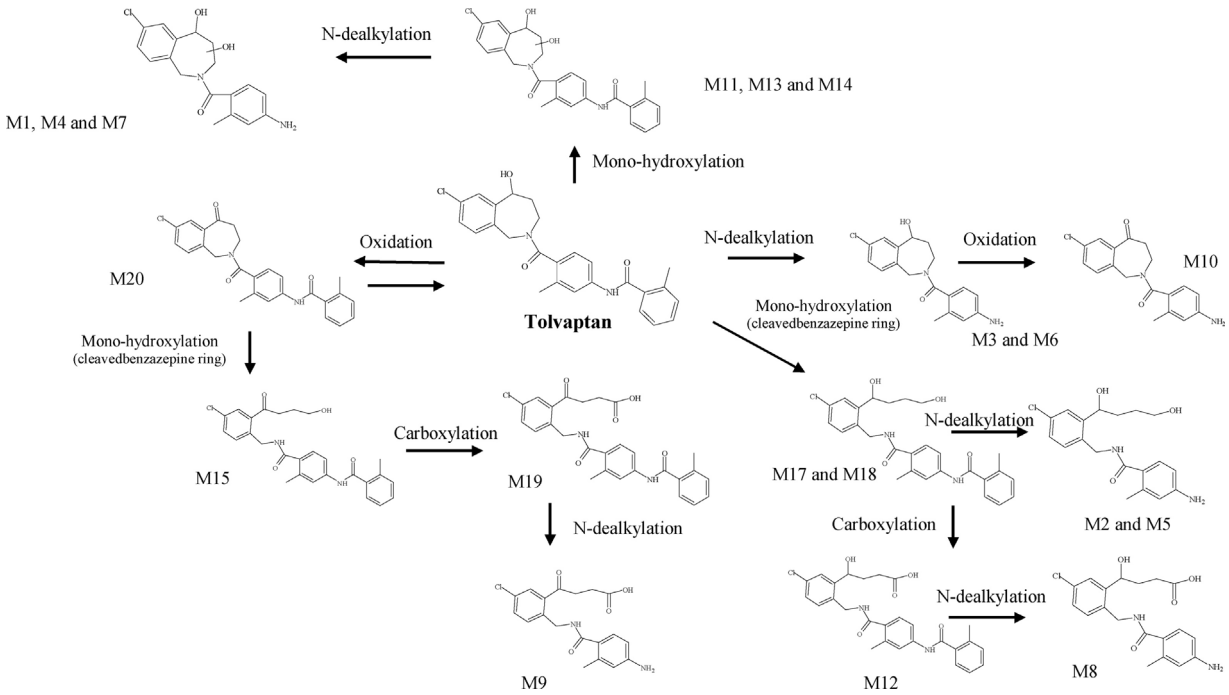

Fig. 3. Scheme of the biotransformation pathways of tolvaptan characterized in this study.

The analysis of the *in vitro* samples using the time-of flight system in full scan acquisition mode allowed the isolation of 16 compounds, all containing the characteristic chlorine isotope pattern (see Table 1 for the elemental composition) and none of them present in the negative control sample obtained incubating tolvaptan in the absence of HLM. Four additional compounds (M8, M9, M10 and M19) were detected using the MRM method here developed (see Fig. 3 for the postulated structures of the compounds detected). The structural elucidation of the detected compounds was conducted on the basis of both the elemental composition and the presence or absence of the representative structural markers selected (characteristic portions of the molecular structure that is common to tolvaptan and its metabolites: *m*/*z* 119, 135, 178 and 252, see again Fig. 1).

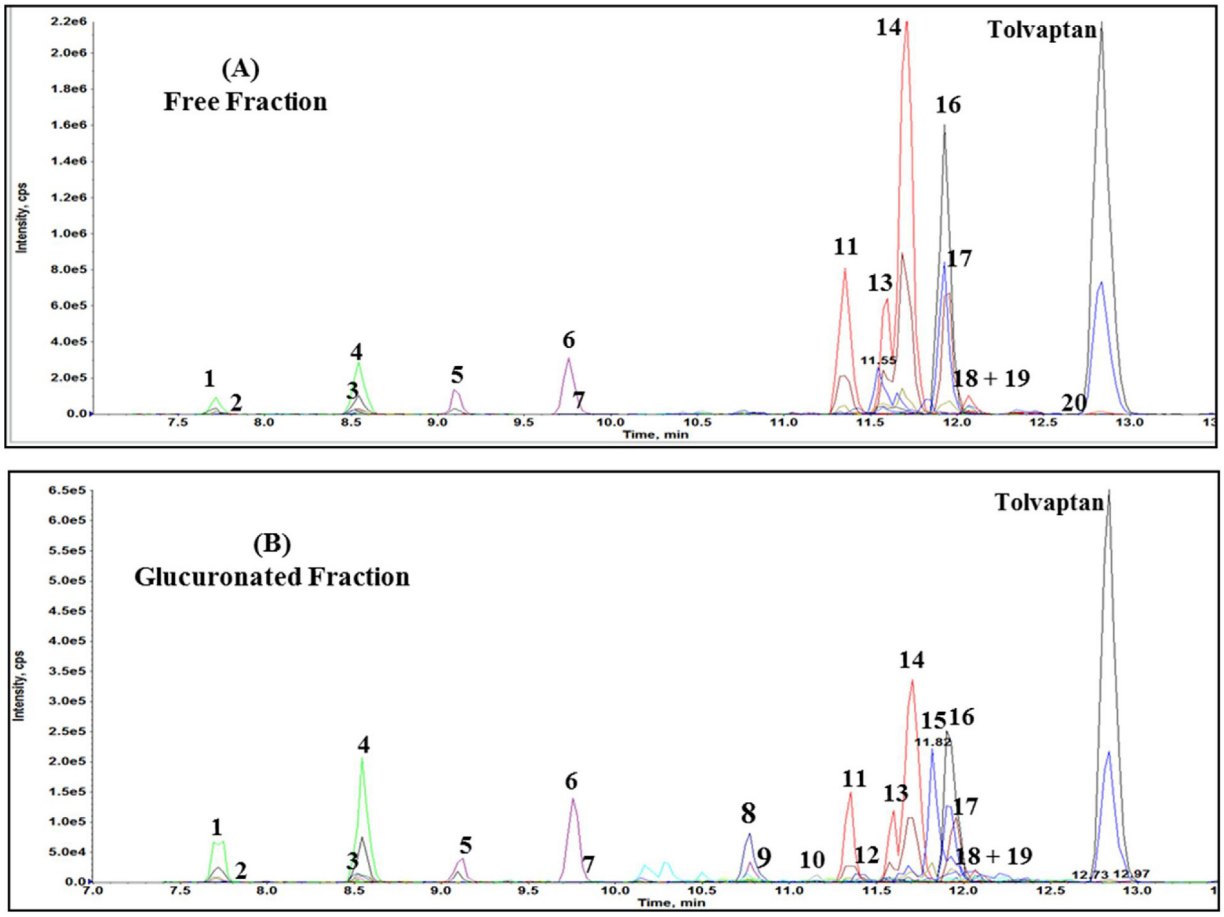

Fig. 4. Extracted chromatograms obtained analyzing the phase I (A) and phase II (B) *in vitro* samples obtained incubating tolvaptan (20 μM) in the presence of HLM. Detection was performed using the SRM method set up in this study.

More in details, the following evidence was obtained by means of the data obtained using both the time-of flight (in full scan and product ion scan as acquisition modes) and the triple quadrupole (in MRM as acquisition mode) systems:

- three chromatographic peaks at retention times of 7.6, 8.6, and 9.8 min (M1, M4 and M7) with elemental composition $C_{18}H_{19}ClN_2O_3$ (MW: 346.1084 Da) and precursor ion at *m*/*z* 347: the absence of the representative structural markers at *m*/*z* 178 and 252, corresponding to the cleavage of the amide bridge between the benzazepine core and the rest of the molecule, and of the fragment ions at *m*/*z* 135 and 119, corresponding to the cleavage at level of the methyl-benzamide core, indicate the cleavage at level of the methyl-benzamide portion; whereas the presence of the fragment ions at *m*/*z* 194 (instead of *m*/*z* 178) and 134 (instead of *m*/*z* 252), indicates hydroxylation of the benzazepine core;
- two chromatographic peaks at retention times 7.7 and 9.1 min (M2 and M5) presenting elemental composition ($C_{18}H_{21}ClN_2O_3$, MW: 348.1241 Da) with two hydrogen atoms more than the dealkylated-hydroxylated metabolites ($C_{18}H_{19}ClN_2O_3$, M1, M4 and M7). Dealkylation together with hydroxylation and cleavage of the benzazepine core were postulated. Confirmation of this assumption rises from the absence of the structural markers at *m*/*z* 119, 135, 178, 194 and 252, together with the presence of the fragment ion at *m*/*z* 134;
- two chromatographic peaks at retention times 8.5 and 9.7 min (M3 and M6) with elemental composition $C_{18}H_{19}ClN_2O_2$ (MW: 330.1135 Da) and precursor ion at *m*/*z* 331. The absence of the structural markers at *m*/*z* 252, 135 and 119 together with the presence of the fragment ion at *m*/*z* 134 (instead of *m*/*z* 252), denote the cleavage at level of the methyl-benzamide portion; whereas the presence of the representative structural marker at *m*/*z* 178 indicates the unmodified benzazepine core;
- one chromatographic peak at retention time 10.7 min (M8) with precursor ion at *m*/*z* 363 and molecular weight 362 Da, 32 Da higher than the dealkylated metabolites (M3 and M6, MW 330 Da). The absence of the representative structural markers at *m*/*z* 178, 252, 135 and 119 together with the presence of the fragment ion at *m*/*z* 134 (instead of *m*/*z* 252), denote the cleavage at level of the methyl-benzamide portion and the modification of the benzazepine core. The difference of 32 Da might be generated either by the presence of two hydroxyl groups or by the cleavage of the benzazepine core with carboxylation. The second option seems to be more probable due to both the retention time and the data reported in literature [19,20].
- one chromatographic peak at retention time 10.8 min (M9) with precursor ion at *m*/*z* 361 and molecular weight 360 Da, 2 Da lower that the dealkylated carboxylated metabolite (M8, MW 362 Da). The cleavage of the benzazepine core with carboxylation and oxidation was postulated;
- one chromatographic peak at retention time 11.2 min (M10) with precursor ion at *m*/*z* 329 and molecular weight 328 Da, 2 Da lower than the dealkylated metabolite (M3 and M6, MW 330 Da). Therefore, the cleavage at level of the methyl-benzamide portion and the oxidation of the hydroxyl group on the benzazepine unit were supposed as the most feasible metabolic modification;

Table 2
Enzymatic isoforms involved in the phase I metabolism of tolvaptan.

ID	Compound	CYP1A2	CYP3A4	CYP3A5	CYP2B6	CYP2C8	CYP2C9	CYP2C19	CYP2D6
M1	*N-dealkylation mono-hydroxylation*	–	+	+	–	–	–	–	–
M2	*N-dealkylation mono-hydroxylation (cleaved benzazepine ring)*	–	+	+	–	–	–	–	–
M3	*N-dealkylation*	–	+	+	–	–	–	–	+
M4	*N-dealkylation mono-hydroxylation*	–	+	+	–	–	–	–	–
M5	*N-dealkylation mono-hydroxylation (cleaved benzazepine ring)*	–	+	+	–	–	–	–	–
M6	*N-dealkylation*	–	+	+	–	–	–	–	+
M7	*N-dealkylation mono-hydroxylation*	–	+	+	–	–	–	–	–
M8	*N-dealkylation carboxylation (cleaved benzazepine ring)*	–	+	+	–	–	–	–	–
M9	*N-dealkylation carboxylation oxidation (cleaved benzazepine ring)*	–	+	+	–	–	–	–	–
M10	*N-dealkylation oxidation*	–	+	+	–	–	–	–	–
M11	*Mono-hydroxylation*	–	+	+	–	–	–	–	–
M12	*Carboxylation (cleaved benzazepine ring)*	–	+	+	–	–	–	–	–
M13	*Mono-hydroxylation*	–	+	+	–	–	–	–	–
M14	*Mono-hydroxylation*	–	+	+	–	–	–	–	–
M15	*Mono-hydroxylation oxidation (cleaved benzazepine ring)*	–	+	+	–	–	–	–	–
M16	*Isomerization*	–	+	+	–	–	–	–	–
M17	*Mono-hydroxylation (cleaved benzazepine ring)*	–	+	+	–	–	–	–	–
M18	*Mono-hydroxylation (cleaved benzazepine ring)*	–	+	+	–	–	–	–	–
M19	*Carboxylation oxidation (cleaved benzazepine ring)*	–	+	+	–	–	–	–	–
M20	*Oxidation*	–	+	+	–	–	–	–	–

- four chromatographic peaks at retention times 11.3, 11.6, 11.7 and 11.8 min (M11, M13, M14 and M15) with elemental composition ($C_{26}H_{25}ClN_2O_4$; MW: 464.1503 Da) presenting one oxygen atom more than tolvaptan ($C_{26}H_{25}ClN_2O_3$). Therefore, hydroxylation was supposed for these compounds. The presence of the representative structural markers at *m/z* 119, 135 and 252 and of the fragment ion at *m/z* 194 (instead of *m/z* 178) for M11, M13 and M14, denotes that hydroxylation involves the benzazepine core. Instead for metabolite M15, the absence of the fragment ions at *m/z* 194 and 178 together with the presence of the representative structural markers at *m/z* 119, 135 and 252, indicate that more than one modification involve the benzazepine unit; hydroxylation together with the cleavage of the benzazepine core and oxidation of the hydroxyl group already present on the benzazepine unit were supposed for this metabolite;
- one chromatographic peak at retention time 11.4 min (M12) with elemental composition ($C_{26}H_{25}ClN_2O_5$; MW: 480.1452 Da) presenting two oxygen atoms more than tolvaptan ($C_{26}H_{25}ClN_2O_3$). Therefore, dihydroxylation or carboxylation associate with reduction could be supposed for this metabolite. The presence of the representative structural marker at *m/z* 252 and the absence of the structural markers at *m/z* 178 indicate that the modification involve the benzazepine unit. Being the retention time of this metabolite higher than the hydroxylated metabolites the cleavage of the benzazepine unit associated with carboxylation were supposed as the most feasible metabolic modifications;
- one chromatographic peak at retention time 11.9 min (M16) presenting the elemental composition of tolvaptan ($C_{26}H_{25}ClN_2O_3$; MW: 448.1554 Da);
- two chromatographic peaks at retention times 12.0 and 12.1 min (M17 and M18) with elemental composition ($C_{26}H_{27}ClN_2O_4$; MW: 466.1659 Da) presenting two hydrogen atoms more than the hydroxylated metabolite ($C_{26}H_{25}ClN_2O_5$). The absence of the fragment ions at *m/z* 194 and 178 together with the presence of the representative structural marker at *m/z* 252, indicate that the modification involves the benzazepine unit. Based on the above considerations hydroxylation together with the cleavage of the benazepine core were supposed for these metabolites;
- one chromatographic peak at retention time 12.1 min (M19) with molecular weith of 478 Da, 2 Da less than metabolite M12 ($C_{26}H_{25}ClN_2O_5$; MW: 480.1452 Da). The cleavage of the benzazepine unit associated with carboxylation and the oxidation of the hydroxyl group already present on the benzazepine unit were supposed for this compound;
- one chromatographic peak at retention time 12.7 min (M20) with elemental composition ($C_{26}H_{23}ClN_2O_3$; MW: 446.1397 Da) presenting two hydrogen atoms less than tolvaptan ($C_{26}H_{25}ClN_2O_3$). Therefore, the detected compound could be assigned as oxidized metabolite.

The phase I biotransformation product formed in highest amount was the dealkylated metabolite (M6) followed by dealkylated mono-hydroxylated (M4), mono-hydroxylated (M11, M13 and M14), mono-hydroxylated oxidized with cleaved benzazepine ring (M15) and carboxylated (M12) metabolites. Furthermore, the phase I metabolites also underwent glucuronidation in our experimental conditions. Fig. 4A–B report the extracted chromatograms obtained by analyzing the phase I and phase II aliquots obtained by the *in vitro* samples: as it can be seen most of the metabolites can be found both in the free and glucuronide fraction, contrarily to what was reported by previous investigators [20].

3.4. Characterization of the enzymatic isoforms involved in the biotransformation pathways of tolvaptan

3.4.1. CYPs

To define the relative contribution of individual CYP isoforms to the overall metabolic rate of observed biotransformation, tolvaptan (at a concentration of 20 μM) was incubated exclusively with each one of the cDNA expressed CYP450 isoforms selected in this study, these being CYP1A2, CYP3A4, CYP3A5, CYP2B6, CYP2C8, CYP2C9, CYP2C19 and CYP2D6. The results obtained are reported in Table 2: CYP450 isoforms mainly involved in the phase I metabolism of tolvaptan are the CYP3A4 and the CYP3A5, confirming the results reported in literature [18]. To confirm these results, tolvaptan was then incubated with pooled human liver microsomes in the presence of different concentration (2, 4, 10 and 20 μM) of a specific inhibitor of the CYP3A subfamily (i.e., ketoconazole). The results of this set of experiments show that in the presence of ketoconazole a significant decrease in the production of the phase I metabolites was registered at all the concentrations evaluated (data not shown), confirming the prominent role of the CYP3A subfamily in the phase I metabolism of tolvaptan.

3.4.2. UGTs

Concerning the characterization of the UGT isoforms involved in the glucuronidation of tolvaptan and its metabolites, the phase I metabolites were extracted from *in vitro* samples and after evapora-

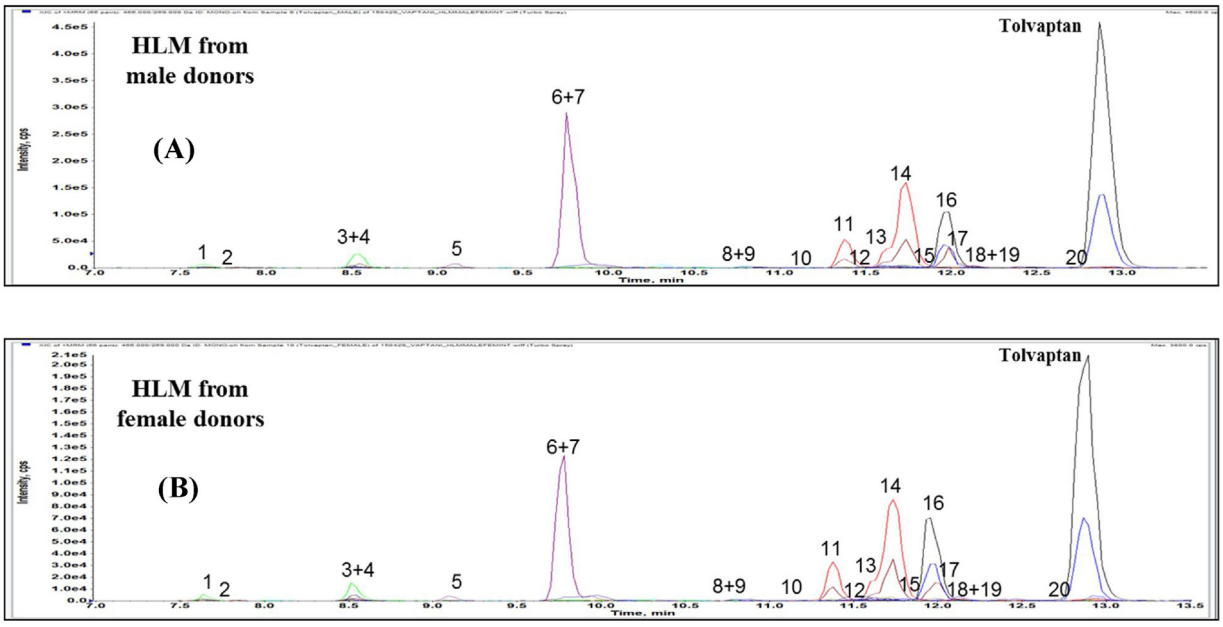

Fig. 5. Extracted chromatograms obtained analyzing the phase I *in vitro* samples after incubation of tolvaptan (20 μM) in the presence of HLM from male donors (A) and from female donors (B). Detection was performed using the SRM method set up in this study.

tion were incubated with exclusively each one of the recombinant human UGT isoforms selected in this study, these being UGT1A1, UGT1A3, UGT1A4, UGT1A6, UGT1A7, UGT1A8, UGT1A10, UGT2B4, UGT2B7, UGT2B10, UGT2B15 and UGT2B17. The results of this set of experiments show for the first time that the isoforms mainly involved in the glucuronidation of tolvaptan are the UGT2B7 (39%) and UGT2B17 (31%), with a minor contribution also from other isoforms.

3.5. Effects of physiological and non-physiological factors on the metabolic profile of tolvaptan

3.5.1. Physiological factors

To investigate the effect of physiological factors (gender and genetic polymorphism) in altering the *in vitro* phase I metabolic profile of tolvaptan, *in vitro* assays were performed incubating tolvaptan (i) in the presence of either HLM exclusively from either female or male donors, to investigate gender differences, (ii) in the presence of HLM containing exclusively the different CYP3A5 allelic variants (without activity CYP3A5 *3*3, moderate activity CYP3A5 *1*3 and high activity CYP3A5 *1*1), to evaluate genetic differences.

Fig. 5A–B report the results obtained analyzing, using the MRM method set up in this study, the samples obtained incubating tolvaptan in the presence of either HLM from female or male donors: as it can be noticed, no appreciable differences were registered in our experimental conditions.

Fig. 6A–C report the results obtained analyzing, using the MRM method set up in this study, the samples obtained incubating tolvaptan in the presence of HLM containing different CYP3A5 allelic variants (without activity CYP3A5 *3*3, moderate activity CYP3A5 *1*3 and high activity CYP3A5 *1*1): as it can be seen, significant differences were registered depending on the specific allelic variant. More in details, in the presence of the allelic variant CYP3A5 *1*1, the formation of the phase I metabolites of second step (e.g., dealkylated hydroxylated metabolites) appeared to be faster if compared to the other CYP3A5 allelic variants (CYP3A5 *3*3 and CYP3A5 *1*3).

3.5.2. Non-physiological factors

To investigate the effect of drug-drug interactions in altering the *in vitro* phase I metabolic profile of tolvaptan, inhibition studies were performed by incubating tolvaptan with either HLM or the cDNA expressed CYP450 isoforms mainly involved in the biotransformation pathways observed (specifically, CYP3A4 and CYP3A5), in the absence and in the presence of the CYP450 inhibitors selected in this study (econazole, ketoconazole, miconazole, tioconazole, gestodene and levonorgestrel), in the same experimental conditions set up in this study. Fig. 7A–C show the results obtained analyzing, using the MRM method here set up, the samples obtained incubating tolvaptan (20 μM) with HLM in the absence (control) and in the presence of different concentrations (2, 4, 10 and 20 μM) of econazole (Fig. 7A), miconazole (Fig. 7B) and tioconazole (Fig. 7C). The levels of all the metabolites were significantly reduced in the presence of all the imidazole antifungals tested, being this effect most evident in the presence of ketoconazole (a well-known inhibitor of the CYP3A subfamily, data not shown) econazole and miconazole, but still significant also in the case of tioconazole. The formation of the metabolites is reduced by more than 50% in the presence of the tested imidazole antifungals at a concentration lower than 2 μM. On the contrary, in the presence of the steroidal progestins the reduction was less evident, and observed only at the highest concentrations studied (data not shown).

4. Conclusions

The analytical strategy and the *in vitro* protocols here proposed, already successfully applied in similar, previous studies, allowed the isolation and mass spectrometric identification of 20 metabolites of tolvaptan, several of which, to the best of our knowledge, never described before. The phase I metabolic reactions include hydroxylation in different positions, oxidation, hydrogenation, dealkylation, carboxylation, isomerization and combinations of the above, being the dealkylated (M6), the dealkylated mono-hydroxylated (M4), the mono-hydroxylated (M11, M13 and M14), the mono-hydroxylated oxidized with cleaved benzazepine ring (M15) and the carboxylated (M12) metabolites the most abundant phase I biotransformation products. The enzymatic isoforms

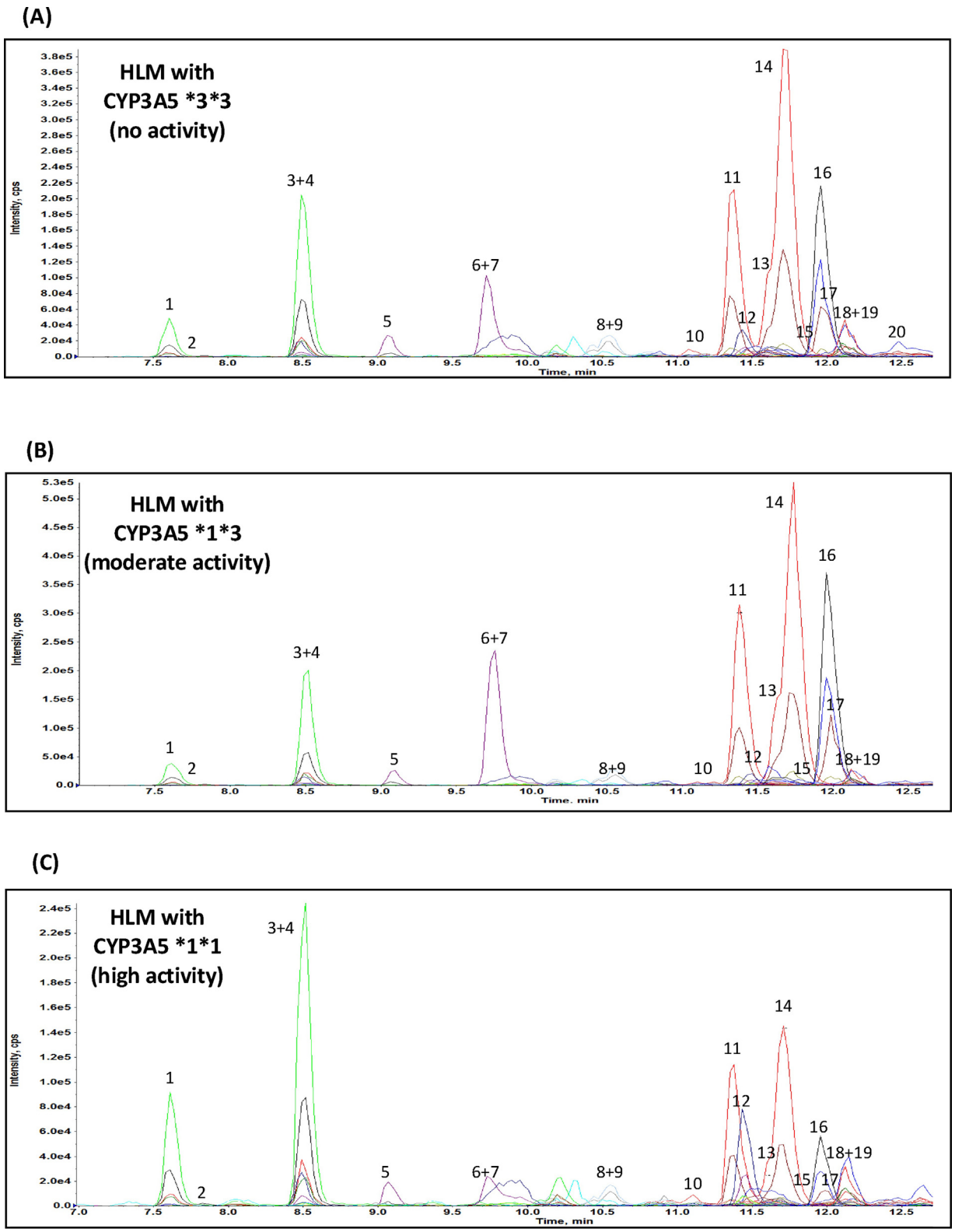

Fig. 6. Extracted chromatograms obtained analyzing the phase I *in vitro* samples after incubation of tolvaptan (20 μM) in the presence of HLM containing the different CYP3A5 allelic variants: without activity CYP3A5 *3*3 (A), moderate activity CYP3A5 *1*3 (B) and high activity CYP3A5 *1*1 (C).Detection was performed using the SRM method set up in this study.

mainly involved in the phase I biotransformation pathways of tolvaptan are the CYP3A4 and the CYP3A5. Once formed, most of the phase I metabolites undergo glucuronidation by UGT2B7 and UGT2B17 isoforms, underlying the necessity to perform enzymatic hydrolysis during the sample preparation or to screen for both the free and conjugate form of the compounds detected. No significant differences in the phase I metabolic profile were registered after incubation of tolvaptan in the presence of either pooled female

or male HLM, showing that the metabolic processes are gender independent, whereas significant differences were registered in presence of HLM containing the different allelic variants of the CYP3A5 isoenzyme.

On the basis of the above results, metabolites M6 and M11-M15, both in the free and in the glucuronated form, appear to be the most suitable urinary diagnostic markers for the detection of tolvaptan intake in doping control.

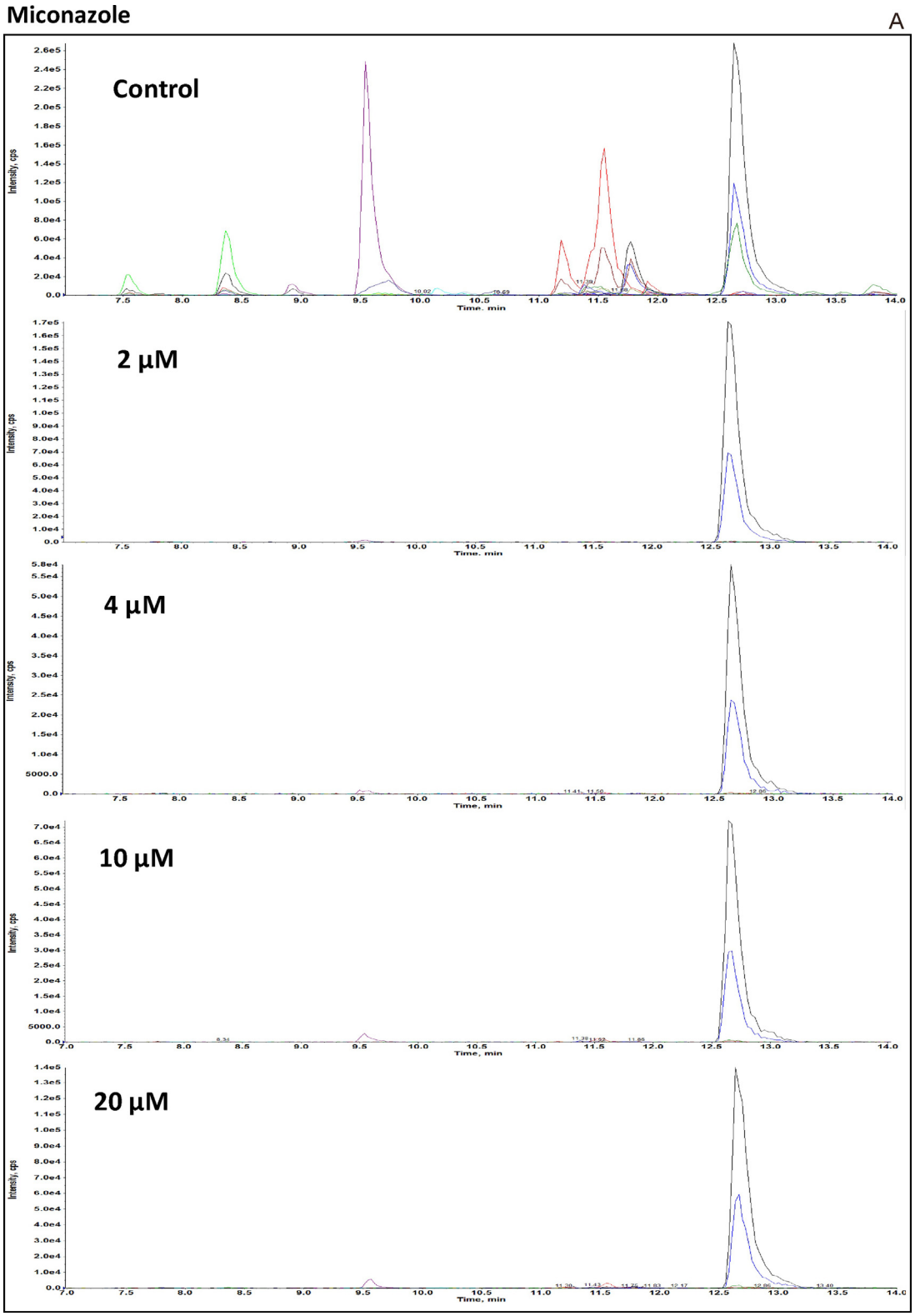

Fig. 7. Extracted chromatograms obtained analyzing the phase I *in vitro* samples after incubation of tolvaptan (20 µM) with human liver microsomes in the absence (control) and in the presence of different concentrations (2, 4, 10 and 20 µM) of econazole (A), miconazole (B) and tioconazole (C). Detection was performed using the SRM method set up in this study.

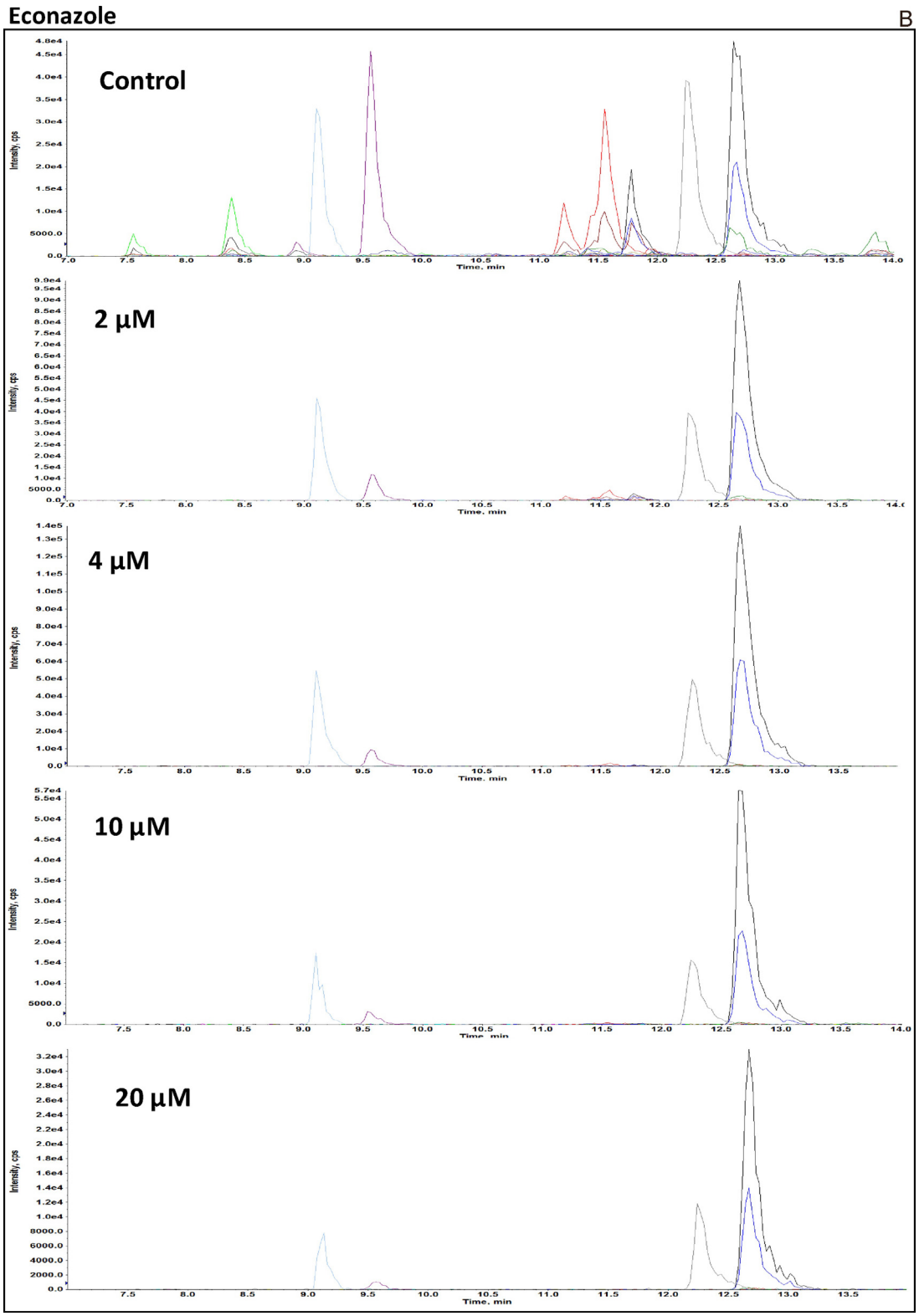

Fig. 7. (*Continued*)

Concerning the effects of drug-drug interactions, significant alterations were registered in the presence of different imidazole antifungals: the metabolic products of tolvaptan were produced in very low levels also at the lowest concentrations of the inhibitors tested, confirming the utility of the screening in urine of the presence of this class of non-prohibited drugs (and/or their diagnostic metabolites) in doping control analysis.

Finally, even if all the chemical structures postulated in this study, based on mass spectrometric data, need to be unambiguously confirmed by additional spectrometric evidence (e.g., NMR spectroscopy of the pure metabolites), nonetheless the results

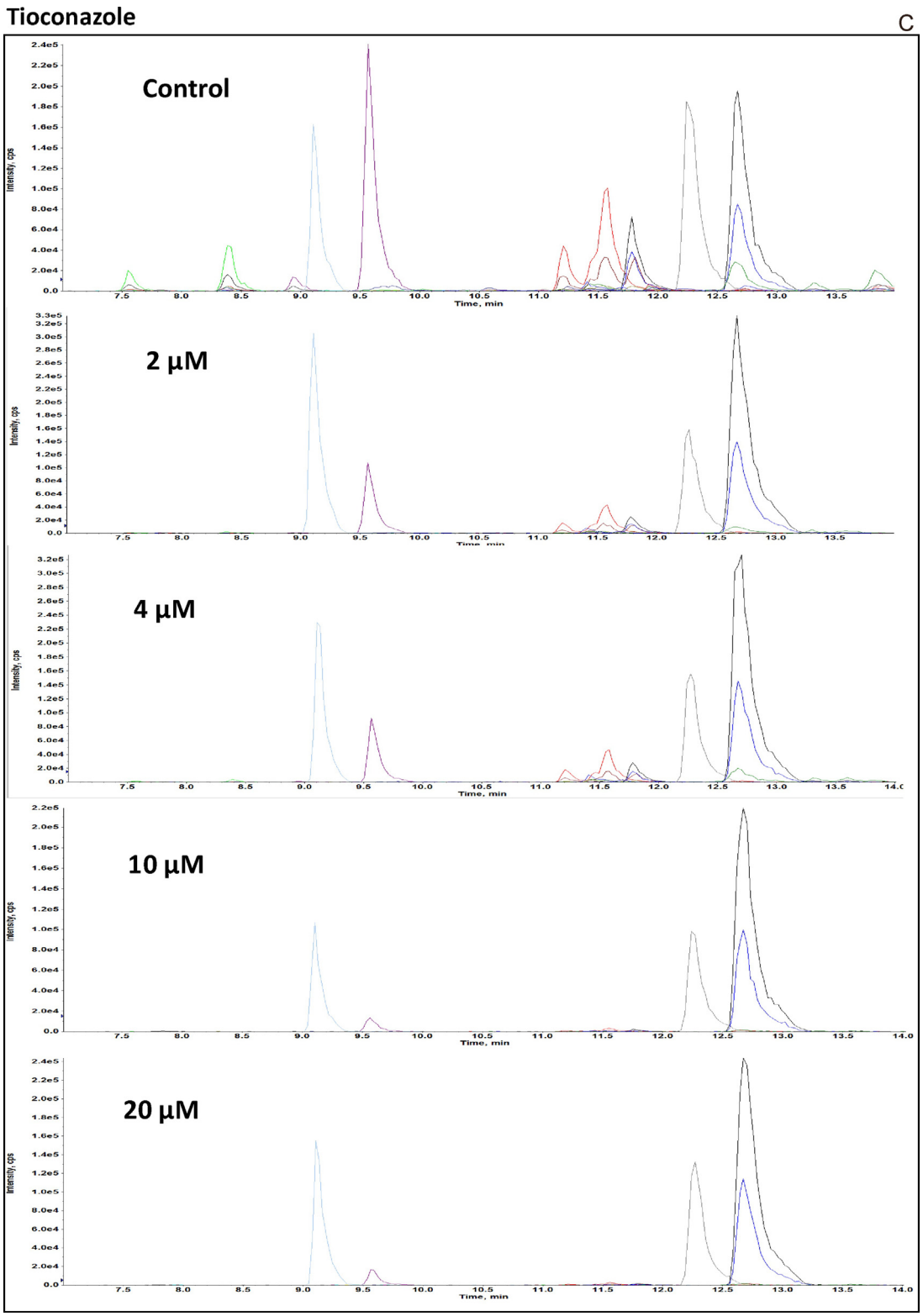

Fig. 7. (*Continued*)

of the current study constitute the basis for a variety of future researches aimed to assess the effects of gender, genetic polymorphisms and drug-drug interactions on the fate of vaptans in the human body. This information will be useful to further refine the selection of the most appropriate marker(s) of administration also in the presence of potential confounding factors (e.g., antifungals). Indeed, as already demonstrated in previous researches carried out in our laboratory [28–31], both genetic polymorphism and drug-drug interactions may not only significantly alter the metabolic profile of the drug, but can also affect the rate of its urinary excretion, leading to significant alteration of the windows of detection of the markers selected to detect its intake. The relevance of the above discussion becomes more evident considering that the enzymes mainly involved in the biotransformation pathways of vaptans are

reported to be either polymorphic (e.g., CYP3A5) or subjected to drug-drug interactions (e.g., CYP3A4), thus underlining that the study of genomic and environmental mechanisms is crucial in the development of the analytical methods utilized in forensic investigations.

Acknowledgements

This project has been supported by a research grant of the World Anti-Doping Agency (WADA) (project code: 15C17MM).

References

[1] F. Ali, M. Guglin, P. Vaitkevicius, J.K. Ghali, Therapeutic potential of vasopressin receptor antagonists, Drugs 67 (2007) 847–858.
[2] G.L. Robertson, Vaptans for the treatment of hyponatremia, Nat. Rev. Endocrinol. 7 (2011) 151–161.
[3] S. Aditya, A. Rattan, Vaptans A new option in the management of hyponatremia, Int. J. Appl. Basic Med. Res. 2 (2012) 77–83.
[4] L.L. Wong, J.G. Verbalis, Vasopressin V2 receptor antagonists, Cardiovasc. Res. 51 (2001) 391–402.
[5] Y. Yamamura, H. Ogawa, H. Yamashita, T. Chihara, H. Miyamoto, S. Nakamura, T. Onogawa, T. Yamashita, T. Hosokawa, T. Mori, M. Tominaga, Y. Yabuuchi, Characterization of a novel aquaretic agent OPC 31260, as an orally effective, nonpeptide vasopressin V2 receptor antagonist, Br. J. Pharmacol. 105 (1992) 787–791.
[6] Y. Yamamura, S. Nakamura, S. Itoh, T. Hirano, T. Onogawa, T. Yamashita, Y. Yamada, K. Tsujimae, M. Aoyama, K. Kotosai, H. Ogawa, H. Yamashita, K. Kondo, M. Tominaga, G. Tsujimoto, T. Mori, OPC-41061, a highly potent human vasopressin V2-receptor antagonist: pharmacological profile and aquaretic effect by single and multiple oral dosing in rats, J. Pharmacol. Exp. Ther. 287 (1998) 860–867.
[7] R.W. Schrier, P. Gross, M. Gheorghiade, T. Berl, J.G. Verbalis, F.S. Czerwiec, C. Orlandi Tolvaptan, a selective oral vasopressin V2-receptor antagonist, for hyponatremia, N. Eng. J. Med. 355 (2006) 2099–2112.
[8] J.-H. Yi, H.-J. Shin, H.-J. Kim, V2 receptor antagonist; tolvaptan, Electrolyte Blood Press. 9 (2011) 50–54.
[9] B.T. Berl, Disorders of fluids and electrolytes: Vasopressin antagonists, N. Eng. J. Med. 372 (2015) 2207–2216.
[10] L.C. Costello-Boerrigter, W.B. Smith, G. Boerrigter, J. Ouyang, C.A. Zimmer, C. Orlandi, J.C. Burnett, Vasopressin-2-receptor antagonism augments water excretion without changes in renal hemodynamics or sodium and potassium excretion in human heart failure, Am. J. Physiol.—Renal Physiol. 290 (2006) F273–F278.
[11] R.W. Schrier, Water and sodium retention in edematous disorders: role of vasopressin and aldosterone, Am. J. Med. 119 (2006) S47–S53.
[12] R. Ventura, J. Segura, Masking and manipulation, in: D. Thieme, P. Hemmersbach (Eds.), Doping in Sports, Handbook of Experimental Pharmacology 195, Springer-Verlag, Berlin Heidelberg, 2010, pp. 327–354.
[13] A.B. Cadwallader, X. de La Torre, A. Tieri, F. Botrè, The abuse of diuretics as performance-enhancing drugs and masking agents in sport doping: Pharmacology, toxicology and analysis, Br. J. Pharmacol. 161 (2010) 1–16.
[14] World Anti-Doping Agency The 2017 Prohibited List. International Standard, Montreal (2017) http://www.wada-ama.org/Documents/World_Anti-Doping_Program/WADA-Prohibited-list/WADA_Prohibited_List_2017_EN.pdf. Last accessed January 2017.
[15] S.E. Shoaf, Z. Wang, P. Bricmont, S. Mallikaarjun, Pharmacokinetics pharmacodynamics, and safety of tolvaptan, a nonpeptide AVP antagonist, during ascending single-dose studies in healthy subjects, J. Clin. Pharmacol. 47 (2007) 1498–1507.
[16] S. Yi, H. Jeon, S.H. Yoon, J. Cho, S.G. Shin, I. Jang, K.S. Yu, Pharmacokinetics and pharmacodynamics of oral tolvaptan administered in 15- to 60-mg single doses to healthy Korean men, J. Cardiovasc. Pharmacol. 59 (2012) 315–322.
[17] S.E. Shoaf, S.R. Kim, P. Bricmont, Pharmacokinetics and pharmacodynamics of single-dose oral tolvaptan in fasted and non-fasted states in healthy Caucasian and Japanese male subjects, Eur. J. Clin. Pharmacol. 68 (2012) 1595–1603.
[18] P.R. Bhatt, E.B. McNeely, T.E. Lin, K.F. Adams, J.H. Patterson, Review of Tolvaptan's pharmacokinetic and pharmacodynamic properties and drug interactions, J. Clin. Med. 3 (2014) 1276–1290.
[19] M. Furukawa, K. Miyata, C. Kawasome, Y. Himeda, K. Takeuchi, T. Koga, Y. Hirao, K. Umehara, Liquid chromatography–tandem mass spectrometry method for determining tolvaptan and its nine metabolites in rat serum: application to a pharmacokinetic study, Arch. Pharm. Res. 37 (2014) 1578–1587.
[20] S. Rzeppa, L.N. Vieta, Analysis of tolvaptan and its metabolites in sports drug testing by high-performance liquid chromatography coupled to tandem mass spectrometry, Drug Test. Anal. 8 (2016) 1090–1094.
[21] F. Botrè, Drugs of abuse and abuse of drugs in sportsmen: The role of in vitro models to study effects and mechanisms, Toxicol. In Vitro 17 (2003) 509–513.
[22] F. Botrè, X. de la Torre, F. Donati, M. Mazzarino, Narrowing the gap between the number of athletes who dope and the number of athletes who are caught: Scientific advances that increase the efficacy of antidoping tests, Br. J. Sports Med. 48 (2014) 833–836.
[23] F. Botrè, Masking and unmasking strategies in sport doping, in: K. Georgakopoulos, M. Alsayrafi (Eds.), Advances and Challenges in Antidoping Analysis, Future Sciences Group, London, UK, 2015, pp. 166.
[24] M. Mazzarino, L. Cesarei, X. de la Torre, I. Fiacco, P. Robach, F. Botrè, A multi-targeted liquid chromatography-mass spectrometry screening procedure for the detection in human urine of drugs non-prohibited in sport commonly used by the athletes, J. Pharm. Biomed. Anal. 117 (2015) 47–60.
[25] J.R. Hill, In vitro drug metabolism using liver microsomes, in: Current Protocols in Pharmacology, John Wiley & Sons, Inc, 2001, pp.
[26] T. Kuuranne, A. Leinonen, W. Schanzer, M. Kamber, R. Kostiainen, M. Thevis, Aryl-propionamide-derived selective androgen receptor modulators: liquid chromatography-tandem mass spectrometry characterization of the in vitro synthesized metabolites for doping control purposes, Drug Metab. Dispos. 36 (2008) 571–581.
[27] M. Mazzarino, M.A. Biava, X. de la Torre, I. Fiacco, F. Botrè, Characterization of the biotransformation pathways of clomiphene, tamoxifen and toremifene as assessed by LC–MS/(MS) following in vitro and excretion studies, Anal. Bioanal. Chem. 405 (2013) 5467–5487.
[28] M. Mazzarino, X. de la Torre, I. Fiacco, A. Palermo, F. Botrè, Drug-drug interaction and doping, part 1: A in vitro study on the effect of non-prohibited drugs on the phase I metabolic profile of toremifene, Drug Test. Anal. 6 (2014) 482–491.
[29] M. Mazzarino, X. de la Torre, I. Fiacco, F. Botrè, Drug-drug interaction and doping, part 2: An in vitro study on the effect of non-prohibited drugs on the phase I metabolic profile of stanozolol, Drug Test. Anal. 6 (2014) 969–977.
[30] A. Palermo, B. Alessi, F. Botrè, X. Torre, I. Fiacco, M. Mazzarino, In vitro evaluation of the effects of anti-fungals, benzodiazepines and non-steroidal anti-inflammatory drugs on the glucuronidation of 19-norandrosterone: Implications on doping control analysis, Drug Test. Anal. 8 (2016) 930–939.
[31] A. Palermo, F. Botrè, X. de la Torre, I. Fiacco, M. Iannone, M. Mazzarino, Drug-drug interactions and masking effects in sport doping: influence of miconazole administration on the urinary concentrations of endogenous anabolic steroids, Forensic Toxicol. 34 (2016) 386–397.